ISSN 1070-3284, Russian Journal of Coordination Chemistry, 2017, Vol. 43, No. 1, pp. 37–43. © Pleiades Publishing, Ltd., 2017.
Original Russian Text © A.N. Gusev, V.F. Shul'gin, I.N. Shcherbakov, K.A. Lysenko, V.V. Minin, I.L. Eremenko, 2017, published in Koordinatsionnaya Khimiya, 2017, Vol. 43, No. 1, pp. 46–53.

New Copper(II) Coordination Compounds with 1,3-Bis(5-(Pyridin-2-yl)-1,2,4-Triazol-3-yl)propane

A. N. Gusev[a, *], V. F. Shul'gin[a], I. N. Shcherbakov[b], K. A. Lysenko[c], V. V. Minin[d], and I. L. Eremenko[d]

[a] *Vernadsky Crimean Federal University, ul. Vernadskogo 4, Simferopol, 295007 Russia*

[b] *Southern Federal University, ul. Bol'shaya Sadovaya 105/42, Rostov-on-Don, 344006 Russia*

[c] *Nesmeyanov Institute of Organoelement Compounds, Russian Academy of Sciences, ul. Vavilova 28, Moscow, 119991 Russia*

[d] *Kurnakov Institute of General and Inorganic Chemistry, Russian Academy of Sciences, Leninskii pr. 31, Moscow, 119991 Russia*

**e-mail: galex0330@gmail.com*

Received June 20, 2016

Abstract—Two new copper(II) complexes with 1,3-bis(5-(pyridin-2-yl)-1,2,4-triazol-3-yl)propane (H_2L), $[Cu_2(HL)Cl_3] \cdot H_2O$ (**I**) and $[Cu(H_2L)](ClO_4)_2$ (**II**), were described. The compounds were characterized by elemental analysis, IR spectroscopy, and magnetochemical data. According to X-ray diffraction data (CIF files CCDC nos. 1497511 (**I**), 1497512 (**II**)), complex **I** is binuclear and the metal cations are bound by the nitrogen atoms of the triazole ring and by the chloride anion. Complex **II** is mononuclear. Analysis of the temperature dependence of the magnetic susceptibility of **I** attests to the antiferromagnetic coupling of paramagnetic centers ($-2J = 18$ cm^{-1}). Exchange channels are analyzed by means of density functional theory (B3LYP/6-311G(d)) using the broken symmetry approach.

Keywords: 1,2,4-triazoles, copper(II), binuclear complexes, X-ray diffraction, exchange interaction, quantum chemical calculations, broken symmetry approach

DOI: 10.1134/S1070328417010043

INTRODUCTION

Coordination compounds formed by 1,2,4-triazole and its derivatives are attracting considerable researchers' attention for the broad range of their physicochemical properties promising for the design of new materials. The spin transitions in iron(II) complexes and photo- and electroluminescence of iridium and osmium complexes with triazoles have been described in detail [1–5]. Copper(II) complexes with pyridyltriazoles are of interest as models for studying the exchange interactions through the heterocyclic bridge and as structural and functional models of natural copper-containing enzymes [6–8]. In most copper(II) exchange clusters reported in the literature, paramagnetic centers are connected by double triazole bridges [9, 10]. The pyridyltriazole coordination compounds in which the central atoms are connected by two different bridging groups are represented by few examples, which considerably restricts the possible search for the composition–structure–property correlations for these systems [11].

The use of spacered heterocycles, i.e., molecules in which two chelatophore moieties are connected by a hydrocarbon spacer, as bridging ligands is an efficient method for the preparation of polynuclear 3*d*-metal complexes with unusual architecture. Previously, it was shows that bis(pyridinetriazolyl)alkanes, a new type of spacered azoles, represent promising scaffolds for the preparation of polynuclear copper(II) complexes [12, 13]. As a continuation of these studies, here we describe the structure and magnetic properties of new copper(II) complexes with 1,3-bis(5-(pyridin-2-yl)-1,2,4-triazol-3-yl)propane (H_2L).

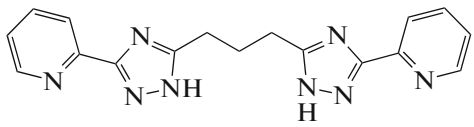

(H_2L)

EXPERIMENTAL

The spacered bistriazole H_2L, which was used as the proligand, was prepared by a previously described procedure [13].

Synthesis of μ-chloro-μ-(3-(5-(pyridin-2-yl-1,2,4-triazolyl)propyl(5-(pyridin-2-yl)-1H-1,2,4-triazolato(—))dichlorodicopper(II) hydrate (I). Copper(II) chloride dihydrate (1 mmol) was added to a solution of H_2L (0.332 g, 1 mmol) in 20 mL of a methanol–water (1 : 1) mixture, and the mixture was magnetically

stirred for 0.5 h until the reactants completely dissolved. Then additional $CuCl_2 \cdot 2H_2O$ (1 mmol) was added and stirring was continued. Several minutes later, a green solid precipitated; the precipitate was left overnight above the mother liquor. Then the crystals were collected on a filter, washed with methanol, and dried in air. Recrystallization from aqueous dioxane afforded 0.320 g of dark green needle crystals. The yield of the complex was 55% relative to triazole.

For $C_{17}H_{17}N_8OCl_3Cu_2$ (M = 582.8)

anal. calcd., %:	C, 35.03;	H, 2.94;	N, 19.22.
Found, %:	C, 34.91;	H, 3.23;	N, 19.21.

Synthesis of (3-(5-(pyridin-2-yl-1,2,4-triazolyl)propyl(5-(pyridin-2-yl)-1H-1,2,4-triazol)copper(II) perchlorate (II). Copper(II) perchlorate hexahydrate (2 mmol) was added to a solution of H_2L (0.332 g, 1 mmol) in 20 mL of methanol and the mixture was magnetically stirred for 1 h until the reactants completely dissolved. The solution was filtered and left for evaporation. After 2/3 of the solution volume evaporated, blue-colored needle crystals formed. The precipitate was separated by filtration and dried. The yield of the complex was 38% in relation to triazole.

For $C_{17}H_{16}N_8O_8Cl_2Cu$ (M = 594.8)

anal. calcd., %:	C, 34.33;	H, 2.71;	N, 19.04.
Found, %:	C, 34.12;	H, 2.68;	N, 19.21.

Elemental analysis for carbon, nitrogen, and hydrogen was performed on a Perkin-Elmer 240 C analyzer.

Thermogravimetric analysis (TGA) was carried out on a Paulik–Paulik–Erdey Q-derivatograph in a static air atmosphere. The heating rate was 5°C/min, a ceramic crucible without a lid served as the sample holder, and calcined alumina was used as the reference.

IR spectra were recorded in a 400–4000 cm^{-1} range on a FSM 2202 FT IR spectrometer using the standard KBr pressed samples.

Magnetochemical measurements were carried out in the 2–300 K range at a 5000 Oe external magnetic field strength during cooling on an MPMS-XL-5 Quantum Design SQUID magnetometer. The diamagnetic contribution was estimated using Pascal's additive method [14]. The magnetic properties were interpreted using the isotropic HDVV spin Hamiltonian: $\hat{H} = -2J \cdot \hat{S}_1 \cdot \hat{S}_2$.

X-ray diffraction. The experimental set of reflections for the single crystals of compounds **I** and **II** were obtained by a standard method [15] on a Bruker SMART APEX II diffractometer equipped with a CCD detector and a monochromatic radiation source (MoK_α, λ = 0.71073 Å). The structures were solved by the direct method and refined in the full-matrix anisotropic approximation for all non-hydrogen atoms. The hydrogen atoms were calculated geometrically and refined in the riding model. The calculations were performed using the SHELX-97 program package [16]. The crystal data and X-ray experiment details are summarized in Table 1 and selected bond lengths are in given Table 2.

The atom coordinates and other parameters of structures **I** and **II** are deposited with the Cambridge Crystallographic Data Centre (nos. 1497511 and 1497512, respectively; deposit@ccdc.cam.ac.uk or http://www.ccdc.cam.ac.uk/data_request/cif).

Quantum chemical calculations were carried out in terms of density functional theory (DFT) using the B3LYP hybrid exchange correlation potential [17] with the exchange part in the form proposed by Becke [18] and the Lee–Yang–Parr correlation part [19]. The extended split valence 6-311G(d) basis set was used. The exchange parameters $-2J$ were calculated using the procedure tested previously [20, 21], which is based on the so-called broken symmetry (BS) approach developed by Ginsberg, Noodleman, and Yamaguchi [22–24].

The exchange parameter was calculated by the formula reported in [25] for the binuclear copper complexes, namely

$$2J = E_{BS} - E_{HS}, \quad (1)$$

where E is the total energy, HS is the high-spin state, and BS is the low-spin state.

The molecular geometry was optimized involving all geometric parameters without symmetry constraints. The BS state energy was calculated at the optimized geometry of the high-spin state. The calculations were carried out using the Gaussian 03 program package [26].

RESULTS AND DISCUSSION

In recent decades, considerable attention has been paid to self-assembly processes during complex formation involving heterocyclic ligands that contain two chelating pyridylazole moieties connected by a hydrocarbon spacer. Quite a number of polynuclear compounds obtained by self-assembly of spacered pyridylpyrazoles with various doubly charged cations have been reported [27–31]. The effect of the spacer on the structure of coordination compounds has been analyzed in detail.

It should be noted, however, that spacered pyridyltriazoles, structurally similar to bis(pyridylpyrazoles), are still poorly studied synthons for the preparation of polynuclear complexes. The copper(II) coordination compounds with bis(pyridyltriazolyl)alkanes obtained at an equimolar reactant ratio or with an excess of the ligand were reported [12, 13]. The reaction of H_2L with

Table 1. Crystallographic data and X-ray experiment and structure refinement details of complexes **I** and **II**

Parameter	Value	
	I	**II**
Temperature, K	150	120
System	Monoclinic	Monoclinic
Space group	$P2_1/n$	$P2_1/c$
Unit cell parameters		
a, Å	7.8760 (5)	12.073(2)
b, Å	16.0268 (9)	38.692(7)
c, Å	16.8937 (10)	14.185(3)
β, deg	98.738 (1)	95.904(6)
V, Å^3	2107.7 (2)	6591(2)
Z	4	12
ρ(calcd.), g/cm^3	1.837	1.798
μ, cm^{-1}	2.43	1.303
F(000)	1168	3612
θ Range, deg	2.4–28.4	1.5–28.1
Index ranges	$-10 \le h \le 10$, $-21 \le k \le 15$, $-22 \le l \le 23$	$-13 \le h \le 15$, $-49 \le k \le 50$, $-18 \le l \le 18$
Unique reflections with $I \ge 2\sigma(I)$	4441	11116
T_{min}/T_{max}	0.626/0.746	0.696/0.781
Refined parameters	288	998
R ($I \ge 2\sigma(I)$)	$R_1 = 0.031$, $wR_2 = 0.096$	$R_1 = 0.0620$, $wR_2 = 0.1547$
$\Delta\rho_{min}/\Delta\rho_{max}$, e Å^{-3}	0.52/−0.34	1.570/−0.968

Table 2. Selected bond lengths for complexes **I** and **II**

Bond	d, Å	Bond	d, Å
I		**II**	
Cu(1)–N(2)	1.944(2)	Cu(1)–N(8)	1.941(4)
Cu(1)–N(1)	2.056(2)	Cu(1)–N(19)	1.965(4)
Cu(1)–Cl(1)	2.2198(7)	Cu(1)–N(21)	2.007(4)
Cu(1)–Cl(3)	2.2713(7)	Cu(1)–N(10)	2.042(4)
Cu(2)–N(3)	1.974(2)	Cu(1)–O(1)	2.433(4)
Cu(2)–N(5)	2.0225(19)	Cu(1)–N(8)	1.941(4)
Cu(2)–N(8)	2.040(2)		
Cu(2)–Cl(2)	2.2944(7)		
Cu(2)–Cl(3)	2.5849(7)		
Cu(1)–N(2)	1.944(2)		

a twofold excess of copper(II) chloride and perchlorate gave previously unknown copper(II) complexes.

According to elemental analysis data, the metal to ligand ratio in coordination compound **I** is 2 : 1. According to TGA data, the complex is stable up to 65°C. Further heating in the 65–110°C range induces a 3% mass loss, corresponding to the removal of one water molecule. Low desolvation temperature and the absence of significant minima in the DTA curve attest to an outer-sphere position of water molecules. Further heating above 300°C leads to decomposition of the complex, continuing as burning-out of its organic part. The IR spectrum of compound **I** exhibits a series of characteristic modes of the ligand. The stretching band of conjugated C=N and C=C bonds of the pyridine ring occurs at 1615 cm^{-1} and is shifted

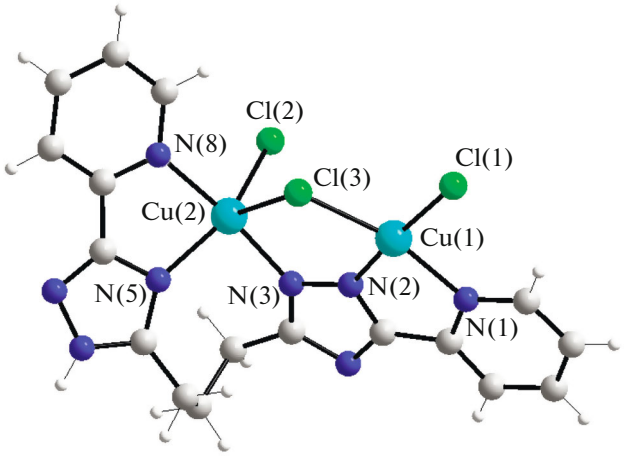

Fig. 1. Molecular structure and atom numbering in complex **I**.

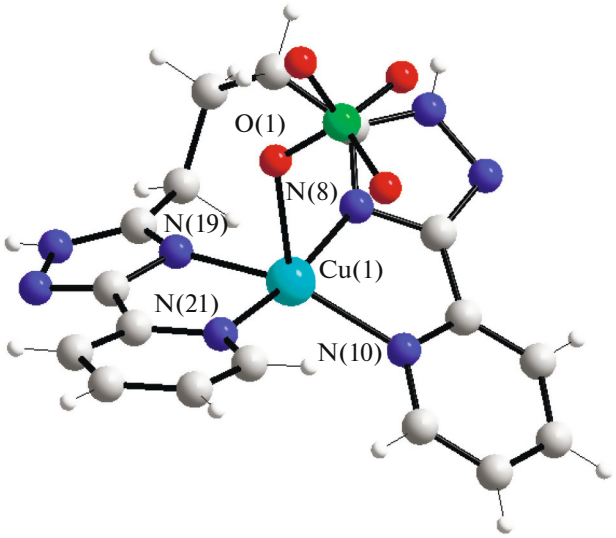

Fig. 2. Structure and atom numbering in complex **II**.

by 12 cm^{-1} to longer wavelengths with respect to the spectrum of the free ligand. The C=N stretching band of the triazole ring is shifted by 7 cm^{-1} to shorter wavelengths from that of the free ligand and is recorded at 1482 cm^{-1}. The 3450–3550 cm^{-1} range has a broad OH stretching band for water molecules involved in the hydrogen bond system.

The structure of complex **I** derived from the X-ray diffraction data is presented in Fig. 1. The complex has a molecular binuclear structure and contains two structurally non-equivalent copper atoms at a distance of 3.779 Å. The copper(II) ions are connected by the chloride anion and μ-N(1)N(2)-triazole ring. The Cu(1) atom is located at the center of a disorder square (the greatest deviation from the root-mean-square plane is 0.129 Å). The Cu(1) coordination sphere is formed by two nitrogen atoms of the Py ring and deprotonated triazole ring and by two chloride anions. The Cu(2) ion is coordinated according to the 4 + 1 mode. The Cu(2) coordination sphere is formed by three nitrogen atoms of the Py ring and two triazole rings and by two chloride anions. The Cu(2) coordination polyhedron is a distorted tetragonal pyramid (τ = 0.42) [32]. The pyramid base is formed by three nitrogen atoms and a chloride anion. The bridging chloride anion is in the axial vertex. The crystal lattice is stabilized by a hydrogen bond system with participation of water molecule (O···N 2.927, O···Cl 3.222, and N···O 2.727 Å).

Complex formation of H_2L with excess copper(II) perchlorate results in crystallization of mononuclear complex **II** (Fig. 2). The independent unit cell contains three cationic complexes differing in the bond parameters and coordination mode of the perchlorate anion. In all three cases, H_2L is coordinated in the tridentate molecular form. The Cu(1) and Cu(2) coordination spheres are formed by four nitrogen atoms of spacered triazole and an oxygen atom of the coordinated monodentate perchlorate anion. The coordination polyhedra are tetragonal pyramids (τ = 0.24 and 0.21). Apart from H_2L, the Cu(3) ion is coordinated by bidentate perchlorate anion, which gives rise to a distorted octahedral environment.

The binuclear copper(II) complexes with binucleating azole ligands attract close attention for the presence of different exchange channels in their molecules. Previously, the attention was focused on binuclear complexes with double pyrazole or triazole bridges. The geometric parameters favorable for antiferromagnetic exchange between the paramagnetic centers were analyzed [10, 11]. However, no reliable data on magnetic behavior – structure correlation in the complexes in which copper(II) ions are double-bridged are available from the literature.

The static magnetic susceptibility of complex **I** in the 14–300 K range follows the Curie–Weiss law with $\theta = -13.85$ K and $C = 0.816$ cm^3 K/mol. At room temperature, the effective magnetic moment of the complex is 2.52 μ_B, which is lower than the expected value for two independent copper(II) ions with $S = 1/2$. As the temperature is lowered, the magnetic moment decreases down to 0.34 μ_B at 5 K, which is indicative of the antiferromagnetic nature of coupling between the paramagnetic centers. The temperature dependence of the magnetic susceptibility (Fig. 3) is adequately described by the Bleaney–Bowers equation with the parameters $g = 2.03$ and $-2J = 18$ cm^{-1}. The obtained antiferromagnetic exchange parameter proved to be unexpectedly low. Numerous experimental data indicate that the magnetic exchange between Cu^{2+} ions through the endocyclic NN' chains (bridging triazole, pyrazole, phthalazine and their derivatives) varies, most often, from moderate to strong [33–

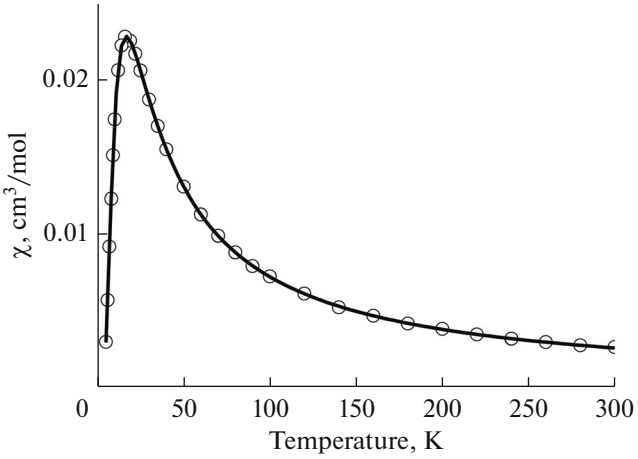

Fig. 3. Temperature dependence of the magnetic susceptibility of complex **I** (continuous line is the theoretical curve).

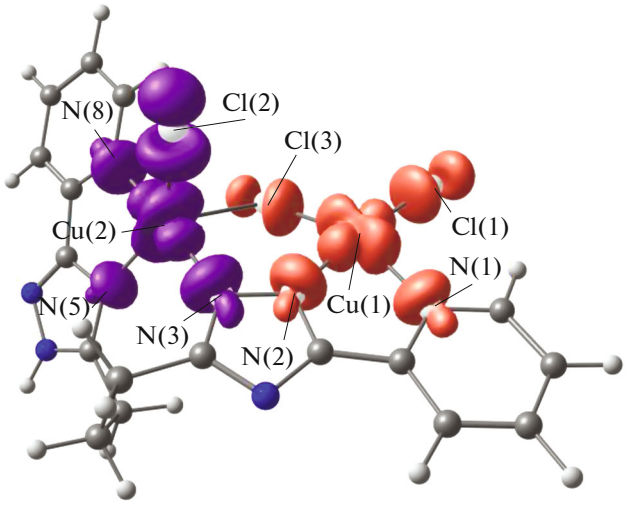

Fig. 4. Spin density distribution in the BS state of complex **I** (the contour value is 0.004 $e/Å^3$).

35]. In order to interpret this fact, quantum chemical modeling of the electronic structure and magnetic exchange in complex **I** was performed.

Since the exchange coupling is fairly sensitive to small geometry changes of the exchanging moieties, we calculated the exchange parameter for the complex in terms of the broken symmetry model for both the X-ray diffraction-derived geometry and the optimized geometry (corresponding to a minimum of the potential energy surface) found for the triplet (HS) electronic state. It was also of interest to follow the possible effect of coordination of a water molecule on the exchange coupling. The calculated exchange parameters for complex **I** and hydrate **I** · H_2O are summarized in Table 3.

As can be seen from the obtained data, the exchange parameter calculated in terms of the broken symmetry approximation has the same sign as the experimental value but the absolute magnitude is overestimated, being in the range $2J = -45...-63$ cm^{-1}. The inclusion of a water molecule in the system affects only slightly the exchange value; therefore, the subsequent analysis was performed using the data on the electronic structure of complex **I** at the optimal geometry, which appears methodically more substantiated. Comparison of the X-ray diffraction-based and calculated geometric parameters of the exchange binuclear moiety is given in Table 4; the atom numbering is similar to that presented in Fig. 1.

As can be seen from the spin density (SD) distribution in the low-spin state of complex **I** (Fig. 4, Table 3), the unpaired electrons of the metal centers are substantially delocalized over the donor atoms of the local coordination environment, the α-density is distributed over Cu(1), N(1), N(2), Cl(1), and Cl(3) atoms, while the β density is on Cu(2), N(3), N(4), N(8), and Cl(2). As a result, the planes that bear electrons with opposite spin moments are rotated relative to each other through a large angle close to 90°, which decreases the antiferromagnetic contribution to the exchange coupling. This SD distribution is determined by magnetically active spin orbits whose calculated shape is shown in Figs. 5a and 5b. The overlap integral of these MOs is quite small (0.0805).

Transition from the high-spin to low-spin state of the complex is accompanied by SD sign inversion on the Cu(2) ion and donor atoms of the Cu(2) coordination sphere, while the SD absolute magnitude remains almost unchanged (Table 5). An exception is the Cl(3)

Table 3. Energies of HS and BS states and calculated exchange parameters ($2J$, cm^{-1}) of complexes **I**, **I** · H_2O, and **III**

Complex	Coordinates	E_{HS}, a.u.	E_{BS}, a.u.	$2J$, cm^{-1}
I · H_2O	XRD	−5756.744370	−5756.744574	−45
I	XRD	−5833.125800	−5833.126032	−51
I · H_2O	Optimized	−5833.400268	−5833.400536	−59
I	Optimized	−5756.940189	−5756.940475	−63
III	*	−5296.246561	−5296.246560	+0.2

*The atom coordinates were taken for the optimized geometry of **I** and the Cl(3) bridging atom was removed.

Table 4. Comparison of the selected geometric parameters of the exchange moiety in complex **I** according to X-ray diffraction (XRD) data and the calculation (B3LYP/6-311G(d))

Bond	XRD	Calcd.	Angle	XRD	Calcd.
	d, Å			α, deg	
Cu(1)–Cu(2)	3.779	3.820	Cu(1)Cl(3)Cu(2)	102.0	100.0
Cu(1)–Cl(3)	2.271	2.321	Cu(1)N(2)N(3)	136.2	135.9
Cu(2)–Cl(3)	2.585	2.659	Cu(2)N(3)N(2)	120.1	121.6
Cu(1)–N(2)	1.944	1.966			
Cu(2)–N(3)	1.974	1.965			

Table 5. Mulliken charges (*q*, *e*) and SD (ρ, *e*) on atoms in the high-spin (HS) and low-spin (BS) states of complex **I**

Atom	HS		BS	
	q, *e*	ρ, *e*	*q*, *e*	ρ, *e*
Cu(1)	1.214	0.668	1.147	0.666
N(1)	–0.583	0.062	–0.568	0.063
N(2)	–0.439	0.064	–0.420	0.066
Cl(1)	–0.651	0.111	–0.591	0.110
Cl(3)	–0.713	0.108	–0.635	0.064
Cu(2)	1.239	0.664	1.122	–0.661
N(3)	–0.469	0.084	–0.436	–0.086
N(4)	–0.580	0.040	–0.590	–0.040
N(8)	–0.594	0.065	–0.570	–0.065
Cl(2)	–0.695	0.118	–0.691	–0.117

bridging, the SD on which decreases almost by half (from 0.108 to 0.064 e) on going from the high- to low-spin state, which is caused by partial overlap of the electron density with opposite spin moment orientation. This suggests that particularly the Cl(3) bridging is responsible for the weak antiferromagnetic coupling observed experimentally for complex **I**.

For estimating the contributions of exchange channels, the exchange parameter was calculated for the hypothetical cation of complex **III**, in which no bridging Cl(3) ion is present, unlike complex **I**. In this structure, the N(2)–N(3) chain of the triazole moiety is the only exchange channel. The exchange coupling in complex **III** is much less pronounced than in **I** and it even becomes weakly ferromagnetic. The calculated exchange parameter is $2J = +0.2$ cm^{-1} (Table 3). The shape of the relevant MOs of the cation of **III** is nevertheless nearly the same as that of complex **I** (Figs. 5c, 5d). However, the overlap integral between these MOs decreases to 0.0429, which is responsible for decreasing antiferromagnetic contribution to the exchange coupling of the metal centers, thus supporting the assumption about the crucial role of the chloride bridge for the exchange transfer.

Thus, quantum chemical calculations indicate that spin density transfer through the chloride bridge is the

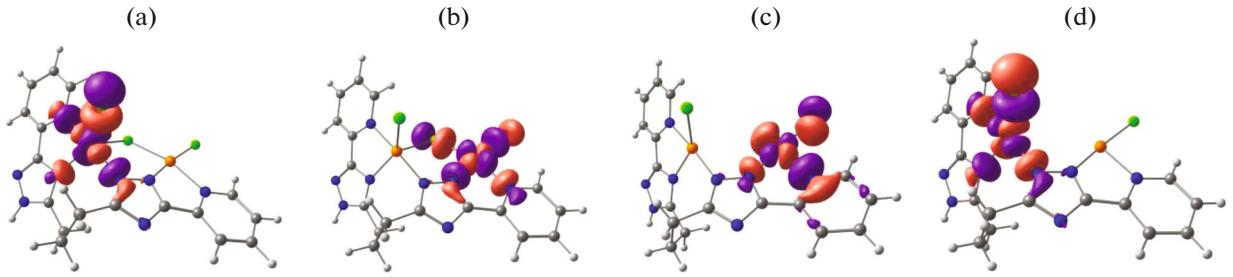

Fig. 5. Localized magnetically active MOs of complexes (a, b) **I** and (c, d) **III**.

most probable exchange mechanism in complex **I**. However, the theoretical exchange parameter is greater than the experimental value, which may be caused by operation of an additional channel through the triazole bridge.

ACKNOWLEDGMENTS

Quantum chemical calculations were carried out at the Center for Collective Use "High Performance Computing" at the Southern Federal University.

This work was supported by the Ministry of Education and Science of the Russian Federation (basic part of the State Assignment in the field of scientific activity, project no. 3874) and the Russian Foundation for Basic Research (grant no. 16-03-00386). The authors are also grateful to the Federal Agency of Scientific Organizations of Russia for financial support.

REFERENCES

1. Haasnoot, J.G., *Coord. Chem. Rev.*, 2000, vols. 200–202, p. 131.
2. Klingele, M.H. and Brooker, S., *Coord. Chem. Rev.*, 2003, vol. 241, p. 119.
3. Kitchen, J.A. and Brooker, S., *Coord. Chem. Rev.*, 2008, vol. 252, p. 2072.
4. Chi, Y. and Chou, P.-T., *Chem. Soc. Rev.*, 2010, vol. 39, p. 638.
5. Park, H.J., Kim, J.N., Yoo, H.-J., et al., *Org. Chem.*, 2013, vol. 78, p. 8054.
6. Roat-Malone R.M., *Bioinorganic Chemistry: A Short Course*, New Jersey: Wiley, 2002.
7. Desbouis, D., Troitsky, I.P., Belousoff, M.J., et al., *Coord. Chem. Rev.*, 2012, vol. 256, nos. 11–12, p. 897.
8. Pauleta, S.R., Dell'Acqua, S., and Moura, I., *Coord. Chem. Rev.*, 2013, vol. 257, no. 2, p. 332.
9. Ouellette, W., Galan-Mascaros, J.R., Dunbar, K.R., et al., *Inorg. Chem.*, 2006, vol. 45, no. 5, p. 1909.
10. Ouellette, W., Prosvirin, A.V., Chieffo, V., et al., *Inorg. Chem.*, 2006, vol. 45, no. 23, p. 9346.
11. Mann, K.L.V., Jeffery, J.C., McCleverty, J.A., et al., *Dalton Trans.*, 1998, p. 89.
12. Gusev, A.N., Shul'gin, V.F., Beyjyyev, E., et al., *Polyhedron*, 2015, vol. 85, p. 525.
13. Gusev, A.N., Nemec, I., Herchel, R., et al., *Dalton Trans.*, 2014, vol. 43, p. 7153.
14. Rakitin, Yu.V. and Kalinnikov, V.T., *Sovremennaya magnetokhimiya* (Modern Magnetochemistry), St. Petersburg: Nauka, 1994.
15. *SMART (control) and SAINT (integration) Sofware. Version 5.0*, Madison: Bruker AXS Inc., 1997.
16. Sheldrick G.M., *SHELXL-97. Program for the Refinement of Crystal Structures*, Göttingen: Univ. of Göttingen, 1997
17. Becke, A.D., *J. Chem. Phys.*, 1993, vol. 98, no. 7, p. 5648.
18. Becke, A.D., *Phys. Rev. A*: *At., Mol., Opt. Phys.*, 1988, vol. 38, no. 6, p. 3098.
19. Lee, C., Yang, W., and Parr, R.G., *Phys. Rev. B: Condens. Matter. Mater. Phys.*, 1988, vol. 37, no. 2, p. 785.
20. Shcherbakov, I.N., Levchenkov, S.I., Tupolova, Y.P., et al., *Eur. J. Inorg. Chem.*, 2013, vol. 2013, no. 28, p. 5033.
21. Levchenkov, S.I., Shcherbakov, I.N., Popov, L.D., et al., *Inorg. Chim. Acta*, 2013, vol. 405, p. 169.
22. Ginsberg, A.P., *J. Am. Chem. Soc.*, 1980, vol. 102, no. 1, p. 111.
23. Yamaguchi, K., Takahara, Y., and Fueno, T., *Applied Quantum Chemistry*, Dordrecht: D. Reidel, 1986.
24. Noodleman, L., Peng, C.Y., Case, D.A., et al., *Coord. Chem. Rev.*, 1995, vol. 144, p. 199.
25. Ruiz, E., Cano, J., Alvarez, S., and Alemany, P., *J. Comput. Chem.*, 1999, vol. 20, no. 13, p. 1391.
26. Frisch, M.J., Trucks, G.W., Schlegel, H.B., et al., *Gaussian 03. Revision E.1*, 2003.
27. Ward, D., *Chem. Commun.*, 2009, p. 4487.
28. Hall, B.R., Manck, L.E., Tidmarsh, I.S., et al., *Dalton Trans.*, 2011, vol. 40, p. 12132.
29. Stephenson, A., Argent, S.P., Riis-Johannessen, T., et al., *J. Am. Chem. Soc.*, 2011, vol. 133, p. 858.
30. Fenton, H., Tidmarsh, I.S., and Ward, M.D., *Dalton Trans.*, 2009, p. 4199.
31. Argent, S.P., Adams, H., Harding, L.P., et al., *New J. Chem.*, 2005, vol. 29, p. 904.
32. Addison, A.W., Rao, T.N., Reedijk, J., et al., *Dalton Trans.*, 1984, p. 1349.
33. Kogan, V.A., Lukov, V.V., and Shcherbakov, I.N., *Russ. J. Coord. Chem.*, 2010, vol. 36, no. 6, p. 401.
34. Popov, L.D., Shcherbakov, I.N., Levchenkov, S.I., et al., *Russ. J. Coord. Chem.*, 2011, vol. 37, no. 7, p. 483.
35. Kogan, V.A., Levchenkov, S.I., Popov, L.D., et al., *Ross. Khim. Zh.*, 2009, vol. 53, no. 1, p. 86.

Translated by Z. Svitanko